Solar Forcing of Drought Frequency in the Maya Lowlands

David A. Hodell,[1]* Mark Brenner,[1] Jason H. Curtis,[1]
Thomas Guilderson[2]

We analyzed lake-sediment cores from the Yucatan Peninsula, Mexico, to reconstruct the climate history of the region over the past 2600 years. Time series analysis of sediment proxies, which are sensitive to the changing ratio of evaporation to precipitation (oxygen isotopes and gypsum precipitation), reveal a recurrent pattern of drought with a dominant periodicity of 208 years. This cycle is similar to the documented 206-year period in records of cosmogenic nuclide production (carbon-14 and beryllium-10) that is thought to reflect variations in solar activity. We conclude that a significant component of century-scale variability in Yucatan droughts is explained by solar forcing. Furthermore, some of the maxima in the 208-year drought cycle correspond with discontinuities in Maya cultural evolution, suggesting that the Maya were affected by these bicentennial oscillations in precipitation.

Lake Chichancanab, on the north-central Yucatan Peninsula, Mexico (Fig. 1), possesses sediments that preserve a highly sensitive record of past climate changes (1, 2). In 1993, we retrieved a 4.9-m sediment core from Lake Chichancanab. The 9000-year-long record of oxygen isotopes and gypsum concentrations from the core was used to infer relative changes in the ratio of evaporation to precipitation (E/P). The record demonstrated that the period 800 to 1000 A.D. was the driest of the middle to late Holocene and that it coincided with the collapse of Classic Maya civilization in the 9th century A.D. The cause of this drought remained elusive, however, although it apparently was widespread in the Neotropics (3–6) and Sahel (7). Here we present analyses from new Lake Chichancanab sediment cores and demonstrate that the terminal Classic drought was only one episode in a recurrent pattern of dry events that occurred during the past 2.6 millennia.

In May 2000, we returned to Lake Chichancanab and retrieved a high-resolution sediment record that enabled us to refine paleoclimatic interpretations for the region over the last 2600 years. Two cores were taken side-by-side in 11 m of water near the deepest area of Chichancanab's central basin. Because uppermost sediments were unconsolidated, the upper 70 cm of each core were extruded vertically in the field and sectioned at 1-cm intervals. Consolidated deposits below 70-cm depth were transported to the laboratory in polycarbonate

tubes, extruded, and sampled at 1-cm intervals for element and stable-isotope analysis. A 1.9-m-long composite section was constructed with the two cores and yielded a basal age of 2600 years before the present (yr B.P.).

Core chronology for the past 2.6 millennia is based on 12 accelerator mass spectrometry (AMS)–^{14}C dates on identifiable terrestrial material (Table 1). This represents a substantial improvement in dating resolution compared with the 1993 core that was studied previously, in which terrestrial material for AMS-^{14}C dating was encountered at only two sediment depths (2). In addition, sedimentation rates in the 2000 core are 40 to 80% greater than those in the 1993 core, averaging 0.7 mm/year from 190- to 85-cm depth and increasing to 0.9 mm/year from 85 cm to the top of the core. Sediment ages above and below 85 cm were calculated with two depth-age linear-regression equations (Table 1). On average, each 1-cm sample represents 11 to 14 years of sediment accumulation.

The Chichancanab core displays considerable stratigraphic variation in the proportions of organic matter, calcium carbonate, and gypsum (Fig. 2, A and B). Lake Chichancanab water is near saturation for gypsum ($CaSO_4$) today (sulfate, 2545 mg liter^{-1}; calcium, 693 mg liter^{-1}), but the mineral precipitates only in shallow water near the lakeshore. During periods of drier climate, lake volume is reduced and $CaSO_4$ saturation is exceeded. Under such dry conditions, gypsum precipitates throughout the entire lake and is preserved in the sediment record, thereby providing a lithologic proxy of past increases in E/P.

Gypsum concentrations in the core were determined by measuring weight percent total S. Gypsum dominates the sediment during three dry periods: 475 to 250 B.C., 125 to 210

A.D., and 750 to 1025 A.D. (Fig. 2B). Yucatan droughts were stronger and more frequent before 1100 A.D., similar to observations in the United States northern Great Plains (8). The oldest arid period occurred between ~475 and 250 B.C. (2500 to 2200 ^{14}C yr B.P.), and previous results from the 1993 Chichancanab core indicated that this event was preceded by a protracted period (~5000 years) of minimal gypsum precipitation and low ^{18}O isotope (δ^{18}O) values, indicating relatively low E/P (2). Evidence for late Holocene climatic drying at ~2500 ^{14}C years B.P., after moist conditions in the early to middle Holocene, is documented throughout the circum-Caribbean. For example, in a core from Lake Miragoane, Haiti, increased aridity at ~2400 ^{14}C yr B.P. was inferred from an increase in δ^{18}O, indicating higher E/P and lower lake levels (9). At the same time, pollen assemblages show a shift from mature mesic forests dominated by Moraceae to dry forest taxa with abundant weeds (10). A similar late Holocene drying trend is detected in sediment cores from Lake Valencia (11), Venezuela, and the offshore Cariaco Basin (6).

The S peak between 125 and 210 A.D. is consistent with pedological and archaeological evidence for a severe dry period at El Mirador, northern Guatemala, that may have contributed to the site's abandonment around 150 A.D. (12). Aridity between 130 and 180 A.D. has also been inferred on the basis of shell δ^{18}O from sediment cores in Lake Salpeten, Guate-
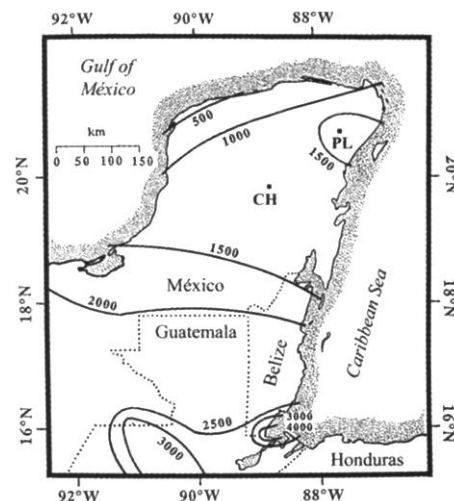

Fig. 1. Location of Lakes Chichancanab (CH) and Punta Laguna (PL) relative to precipitation (mm/year) on the Yucatan Peninsula. Mean annual temperature and rainfall near Lake Chichancanab average 25.4°C and ~1300 mm, respectively, and most of the precipitation occurs during the rainy season between May and September. Mean annual temperature and rainfall near Lake Punta Laguna average 25.7°C and ~1520 mm, respectively. Annual evaporation losses are considerable (1521 mm/year measured at Santa Rosa, 12 km from Lake Chichancanab) at both locations and, consequently, the lake volumes and dissolved solute concentrations are highly sensitive to changes in E/P.

[1]Department of Geological Sciences, University of Florida, Gainesville, FL 32611, USA. [2]Center for Accelerator Mass Spectrometry, Lawrence Livermore National Laboratory, Livermore, CA 94551, USA.

*To whom correspondence should be addressed. E-mail: dhodell@geology.ufl.edu

mala (13). This dry period coincides with pervasive Preclassic site abandonment in the Maya Lowlands (14) that may have been a response to widespread drought on the Yucatan Peninsula (15).

The most recent episode of gypsum deposition (750 to 1025 A.D.) supports our previous finding of prolonged drought between ~800 and 1000 A.D. (2, 16), which coincided with the Classic Maya collapse (15, 17). The density record, which reflects the presence of gypsum, suggests two distinct events centered on 800 A.D. (terminal Classic) and 1020 A.D. (Fig. 2B), similar to the $\delta^{18}O$ record from nearby Lake Punta Laguna (16). Evidence for drier climate from other areas in Mexico, Central America, and northern South America indicates that the terminal Classic drought was widespread (3–6). Two distinct rainfall minima between ~800 and 1000 A.D. have also been documented in the Sahel and coincided with the terminal Classic drought in Yucatan (7, 18, 19). The circum-Caribbean and the Sahel are directly linked through the seasonal migration of the Atlantic intertropical convergence zone, and this correspondence is not surprising (20, 21).

The ratio of ^{18}O to ^{16}O in a tropical closed-basin lake is controlled mainly by E/P because of the preferential loss of ^{16}O from lake water during evaporation. The $\delta^{18}O$ of the water is recorded in the shells of ostracods and gastropods, which precipitate their shells at a constant offset from oxygen isotopic equilibrium that is species-specific (22). The $\delta^{18}O$ record from Chichancanab generally supports our E/P inferences based on the S record. Oxygen isotope values are greater than average between 800 and 1090 A.D. (Fig. 2C) when S content is high. Maximum $\delta^{18}O$ values in this interval are not substantially greater than in other parts of the record, but low $\delta^{18}O$ values (<2.5‰) are conspicuously absent. Similarly, high S content between ~475 and 250 B.C. is associated with elevated mean $\delta^{18}O$ values that decrease rather abruptly at about 150 B.C. Curiously, the S peaks between 125 and 210 A.D. are not associated with high average $\delta^{18}O$ values, and the corresponding density peaks in this period are not as high as those recorded in some of the other drought events (Fig. 2B).

Firm sediments below 70 cm were analyzed in their polycarbonate core tubes with a GEOTEK MultiSensor Core Logger (MSCL). Gamma-ray attenuation (GRA) was measured at 0.5-cm intervals and converted to sediment bulk density with a water-aluminum calibration standard. The GRA bulk density stratigraphy is nearly identical to the weight % S profile (Fig. 2B), because authigenic gypsum is denser than the shell-bearing organic matter that composes most of the sediment core. The double peak in density (gypsum) between 750 and 1000 AD may have blurred when the core was extruded and sampled because of the difficulty in sectioning the dense nodular gypsum in this inter-

val. Consequently, the weight % S measured on discrete samples shows a single, broad high rather than two distinct peaks between 750 and 1000 A.D.

Because the density record is at higher resolution (0.5-cm intervals) than either the weight % S or $\delta^{18}O$ record and was measured on

whole cores before extrusion and sampling, we used it for time series analysis. Spectral analysis of the density signal revealed power concentrated at periods of ~810, 208, 100, 50, and 39 years (Fig. 3A). The peak at 208 years dominates the spectrum and is significant at the 95% confidence level, whereas the peaks at 50 and
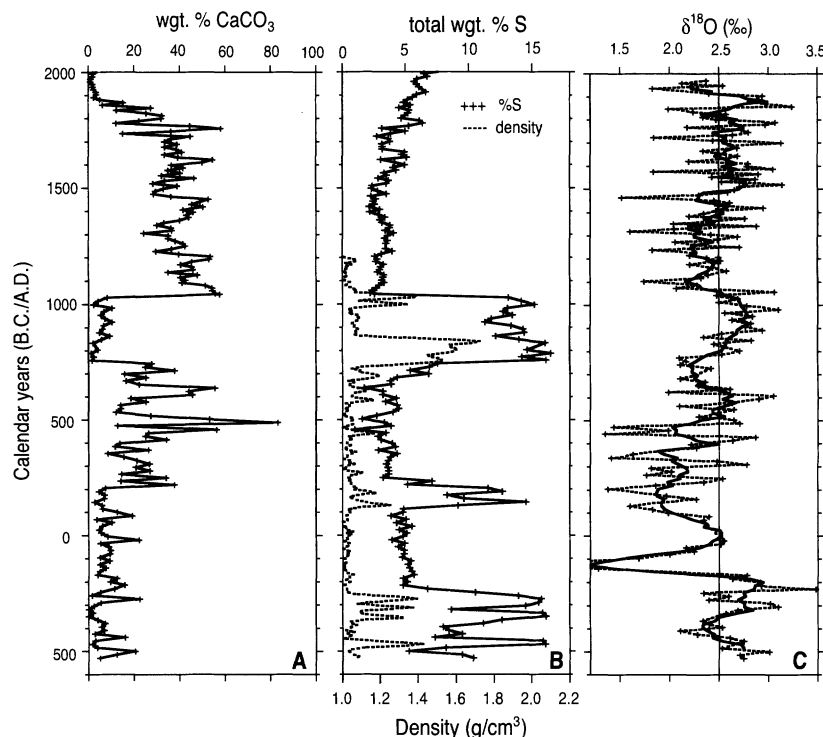

Fig. 2. Element and isotope results from Chichancanab core CH-23-V-00 versus calendar year (B.C./A.D.). **(A)** Weight % carbonate determined by coulometric titration (35). **(B)** Weight % total S (solid line) measured with a Carlo Erba CNS analyzer and gamma-ray attenuation bulk density (dashed line) measured with a GEOTEK Multi-Sensor Core Logger. **(C)** $\delta^{18}O$ of the gastropod *Pyrgophorus coronatus* (36). Dashed line and crosses correspond to the raw data and bold line represents a five-point running mean through the data. Vertical line at 2.5‰ is the mean value of all data.

Table 1. Age analysis of sediment core CH-23-V-00 from Lake Chichancanab. Radiocarbon analyses were performed solely on terrestrial organic matter (seed, charcoal, carbonized wood fragments) because aquatic materials are subject to significant hard-water lake error associated with the dissolution of limestone bedrock (devoid of ^{14}C) in the karst watershed of Chichancanab. Radiocarbon dates were converted to calendar years with the program OxCal version 3.5 (33) and atmospheric data from Stuiver et al. (34). Sediment depths were converted to age with two equations derived by linear regression of depth-age points above and below 85 cm. 0 to 85 cm: age (cal yr B.P.) = −10.276 + 10.563 × depth (cm), sedimentation rate = 0.09 cm/year, r^2 = 0.999; 85 cm to bottom: age (cal yr B.P.) = −388.18 + 15.15 × depth (cm), sedimentation rate = 0.07 cm/year, r^2 = 0.993.

Sample ID	Depth (cm)	Composite depth (cm)	Accession number	Age (^{14}C yr B.P.)	Error (± yrs)	Age (cal yr B.P.)
CH 23-V-00 2B	42–44	42	CAMS-68115	370	50	410*
CH 23-V-00 2B	72–73	72	CAMS-68116	890	100	815
CH 23-V-00 2B	75–79	75	CAMS-68117	860	70	795*
CH 23-V-00 2B	81–82	81	CAMS-68118	870	50	800
CH 23-V-00 2B	87–89	87	CAMS-68119	990	60	870*
CH 23-V-00 1B	99–100	105	CAMS-69152	1350	50	1260*
CH 23-V-00 1B	100–101	106	CAMS-69153	1350	50	1260*
CH 23-V-00 2B	136–137	136	CAMS-68122	1770	50	1690*
CH 23-V-00 2B	139–140	139	CAMS-68123	1800	60	1715*
CH 23-V-00 2B	145–146	145	CAMS-69154	1830	80	1740*
CH 23-V-00 2B	147–148	147	CAMS-69155	1840	140	1775
CH 23-V-00 2B	183–184	183	CAMS-69156	2310	110	2400*

*Denotes dates that were used for regressions.

39 years are significant at the 80% level. The periods near ~100 and 50 years may be harmonics of the ~208 year cycle. Time series analysis of the $\delta^{18}O$ record from Lake Punta Laguna (16), located ~150 km northeast of Chichancanab, also reveals a 208-year cycle over the last 2000 years (Fig. 3B) that is coherent and in phase with the density record from Chichancanab (Fig. 4B). A 200-year cycle has also been noted in foraminifera abundance records from the Cariaco Basin off Venezuela and is attributed to solar forcing of century-scale variability in regional upwelling and trade-wind intensity during the Holocene (23).

A 206-year cycle is prevalent in records of cosmogenic nuclide production including both ^{14}C and ^{10}Be (Fig. 3) (24, 25), and is believed to reflect solar variability or a combination of solar forcing and oceanic response. Periods of higher solar activity correspond to times of lower cosmonuclide production. Comparison of the Punta Laguna $\delta^{18}O$ and the ^{14}C production ($\Delta^{14}C$) records shows an antiphase relation for the past 2000 years (Fig. 4) (25). Higher E/P ($\delta^{18}O$) coincides with lower ^{14}C production, implying that drought occurred during times of increased solar activity (Fig. 4). A similar relation between drought and high solar radiation has been demonstrated in lake sediment records from equatorial east Africa that span the past 1100 years (26).

The mechanism by which changes in solar activity cause E/P shifts in Yucatan is not certain. An amplifying mechanism is required to obtain a significant climate response from rather small variations in solar output (27). Hypothesized mechanisms include changes in the ultraviolet part of the solar spectrum, which affects ozone production and stratospheric temperature structure (28), and the effect of cosmic ray intensity on cloud formation and precipitation (29). Sensitivity experiments conducted with atmospheric general circulation models imply that changes in solar output may affect global mean temperature, humidity, convection, and intensity of Hadley circulation in the trop-
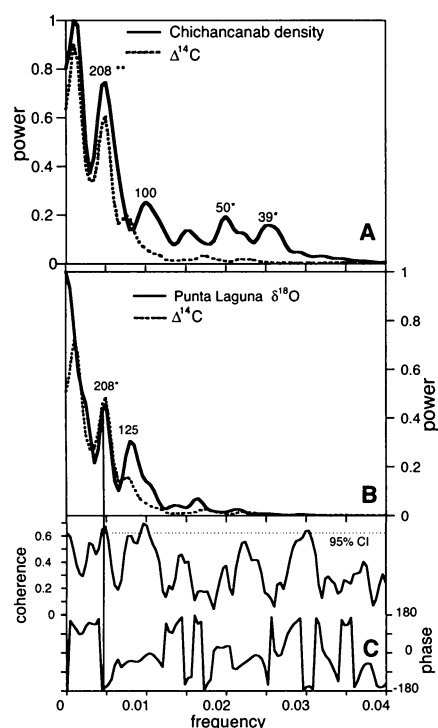
Fig. 3. (A) Power spectra of Chichancanab GRA bulk density record (black line) and $\Delta^{14}C$ for the last 2500 years (dashed gray line) (34). **(B)** Power spectra of the $\delta^{18}O$ signal measured on the ostracod *Cytheridella ilosvayi* in a sediment core from Lake Punta Laguna (black line) (16) and $\Delta^{14}C$ (dashed gray line) (34). Power spectra were calculated with the program Analyseries (37) by interpolating the signals at uniform 5-year intervals and linear detrending. All estimates were made with a Bartlett window, 1/3 lag, and no prewhitening constant was applied. (**) Denotes peaks in the GRA bulk density and $\delta^{18}O$ signals that are significant at the 95% confidence level; (*) denotes significance at the 80% level. The peak at a period of ~208 years dominates the spectra of E/P proxies in Yucatan and $\Delta^{14}C$ (34), suggesting that the 208-year drought cycle on the Yucatan Peninsula is related to variations in solar activity. **(C)** Coherency and phase from cross-spectral analysis of the Punta Laguna $\delta^{18}O$ and $\Delta^{14}C$ signals. The signals are coherent (~0.7) and ~180° out of phase at the 208-year period.

Fig. 4. (A) Comparison of $\Delta^{14}C$ (red line) (30), $\delta^{18}O$ record from Lake Punta Laguna (black line) (16), and GRA bulk density from Lake Chichancanab (blue line). Peaks in $\delta^{18}O$ indicate increased E/P (drought) and coincide with minima in ^{14}C production that are caused, in part, by increased solar activity (38). M, S, and W denote the Maunder, Sporer, and Wolf sunspot minima, respectively. **(B)** Bandpass filter centered at 208-years of the $\Delta^{14}C$ record (red line) (34), $\delta^{18}O$ signal from Lake Punta Laguna (black line) (16), and the GRA bulk density signal from Lake Chichancanab (blue line). The 208-year filtered component of $\delta^{18}O$ is in phase with inferred solar variability (or 180° out of phase with $\Delta^{14}C$ production) for the last 1500 years. The 208-year component of the Punta Laguna $\delta^{18}O$ and Chichancanab density signals are in phase between 0 and 1200 A.D.
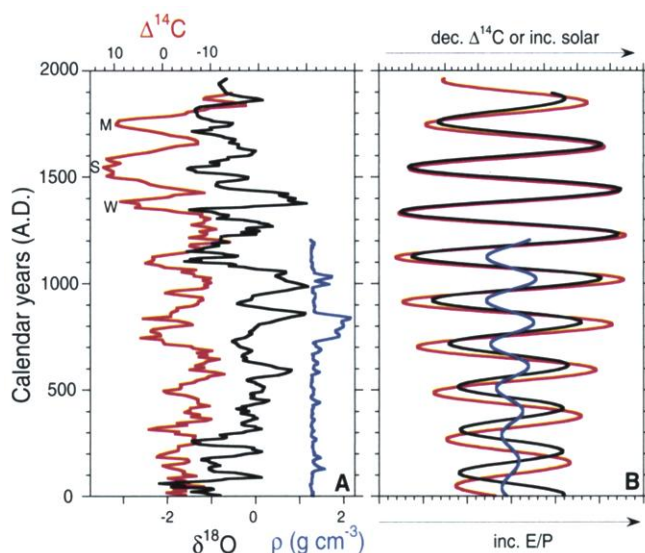
Fig. 5. (A) GRA bulk density record from Lake Chichancanab (black line) shown relative to a bandpass filter (dashed gray line) of the signal centered at ~50 years (frequency = 0.02 ± 0.005). **(B)** GRA bulk density record from Lake Chichancanab (black line) shown relative to a bandpass filter (dashed gray line) of the signal centered at ~208 years (frequency = 0.0048 ± 0.0008). Centennial-scale Yucatan droughts recurred at a period of ~208 years and were often composed of multidecadal oscillations with a period near 50 years. Shown to the right are the subdivisions of Maya cultural evolution. Some of the drought events coincide with important Maya cultural discontinuities such as the Preclassic Abandonment (PA) between 150 and 200 A.D. and the Terminal Classic Collapse (TC) between 750 and 900 A.D.
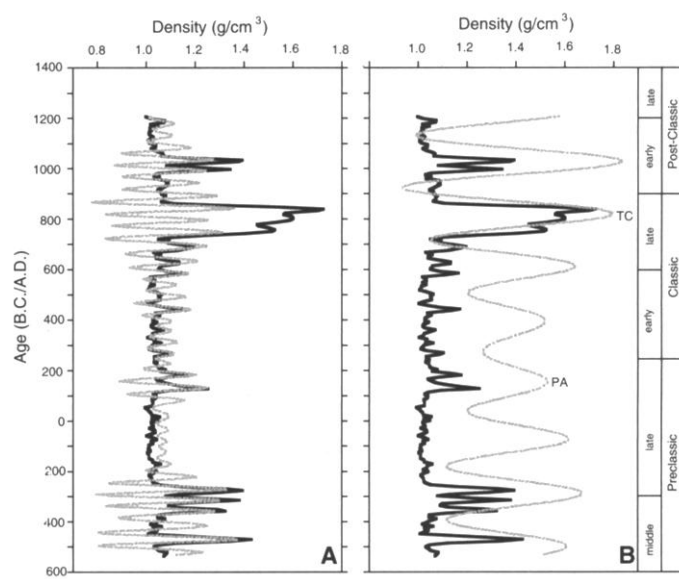
ics (30–32). Mean annual rainfall on the Yucatan Peninsula varies by a factor of 5 over a distance of only ~500 km between the semiarid northwest coast (500 mm/year) and the southern lowlands of northern Guatemala and Belize (2500 mm/year) (Fig. 1). Consequently, any solar-forced change in the strength or position of Hadley circulation or tropical convective activity would be expected to affect rainfall in the region.

A comparison of the Chichancanab GRA bulk density record with bandpass filters of the signal, centered at periods of 50 and 208 years, shows that the large bicentennial-scale drought events were often composed of multiple ~50-year oscillations. The record demonstrates that the arid events centered at 485 B.C. and 285 B.C. were part of the 208-year cycle (Fig. 5). Similarly, the droughts between 125 and 210 A.D. (associated with Preclassic Abandonment), at ~800 A.D. (associated with terminal Classic Collapse), and ~1020 A.D. also fit the pattern of 208-year drought recurrence. The Maya were highly dependent on rainfall and surface reservoirs as their principal water supply (15). Consequently, these multidecadal- to multicentury-scale oscillations in precipitation probably had a detrimental impact on Maya food production and culture.

References and Notes

1. A. Covich, M. Stuiver, Limnol. Oceanogr. 19, 682 (1974).
2. D. A. Hodell, J. H. Curtis, M. Brenner, Nature 375, 391 (1995).
3. S. E. Metcalfe, Holocene 5, 196 (1995).
4. S. E. Metcalfe et al., in Environmental Change in Drylands: Biogeographical and Geomorphological Perspectives, A. C. Millington, K. Pye, Eds. (Wiley, Chichester, UK, 1994), pp. 131–145.
5. S. P. Horn, R. L. Sanford, Biotropica 24, 354 (1992).
6. G. H. Haug, K. A. Hughen, D. M. Sigman, L. C. Peterson, U. Rohl, in preparation.
7. F. A. Street-Perrott et al., Holocene 10.3, 293 (2000).
8. K. R. Laird, S. C. Fritz, K. A. Maasch, B. F. Cumming, Nature 384, 552 (1996).
9. D. A. Hodell et al., Nature 352, 790 (1991).
10. A. Higuera-Gundy et al., Quat. Res. 52, 159 (1999).
11. J. P. Bradbury et al., Science 214, 1299 (1981).
12. B. H. Dahlin, Clim. Change 5, 245 (1983).
13. M. F. Rosenmeier et al., in preparation.
14. R. D. Hansen, Excavations in the Tigre Complex, El Mirador, Peten, Guatemala (New World Archaeological Foundation, Bringham Young University, Provo, UT, 1990).
15. R. B. Gill, The Great Maya Droughts: Water, Life, and Death (Univ. of New Mexico Press, Albuquerque, NM, 2000).
16. J. H. Curtis, D. A. Hodell, M. Brenner, Quat. Res. 46, 37 (1996).
17. J. W. G. Lowe, The Dynamics of Apocalypse (Univ. of New Mexico Press, Albuquerque, NM, 1985).
18. J. A. Holmes, M. Allen, F. A. Street-Perrott, R. A. Perrott, Palaeogeogr. Palaeoclimatol. Palaeoecol. 148, 169 (1999).
19. F. Gasse, E. Van Campo, Earth Planet. Sci. Lett. 126, 435 (1994).
20. S. H. Hastenrath, J. Atmos. Sci. 33, 202 (1976).
21. _____, E. B. Kaczmarczyk, Tellus 33, 453 (1981).
22. U. von Grafenstein, H. Erlernkeuser, P. Trimborn, Palaeogeogr. Palaeoclimatol. Palaeoecol. 148, 133 (1999).
23. L. C. Peterson, J. T. Overpeck, N. G. Kipp, J. Imbrie. Paleoceanography 6, 99 (1991).
24. M. Stuiver, T. F. Braziunas, Holocene 3.4, 289 (1993).
25. G. M. Raisbeck, F. Yiou, J. Jouzel, J. R. Petit, Philos. Trans. R. Soc. London 330, 463 (1990).
26. D. Verschuren, K. R. Laird, B. F. Cumming, Nature 403, 410 (2000).
27. Reviewed in J. Beer, W. Mende, R. Stellmacher, Quat. Sci. Rev. 19, 403 (2000).
28. J. D. Haigh, Nature 370, 544 (1994).
29. B. Van Geel et al., Quat. Sci. Rev. 18, 331 (1999).
30. D. Rind, J. Overpeck, Quat. Sci. Rev. 12, 357 (1994).
31. _____, in Natural Climate Variability on Decade-to-Century Time Scales, D. G. Martinson et al., Eds. (National Academy Press, Washington, DC, 1995), pp. 187–198.
32. G. C. Reid, K. S. Gage, in Secular Solar and Geomagnetic Variations in the Last 10,000 Years, F. R. Stephenson, A. W. Wolfendale, Eds. (Kluwer, Dordrecht, Netherlands, 1988), pp. 225–244.
33. C. Bronk Ramsey, Radiocarbon 40, 461 (1998).
34. M. Stuiver et al., Radiocarbon 40, 1041 (1998).
35. E. E. Englemann, L. L. Jackson, D. R. Norton, Chem. Geol. 53, 125 (1985).
36. About 10 to 15 specimens were selected from each 1-cm sample. Each shell was cracked open and sonicated in methanol to remove fine-grained particles that fill the chambers. Cleaned shell fragments were treated with 15% H_2O_2 for 1 hour to remove organic matter, dried, and ground to a homogenous powder. Stable isotopes were analyzed at the University of Florida with a Kiel III carbonate preparation device interfaced with a Finnigan MAT 252 mass spectrometer. Results are reported in standard delta notation ($\delta^{18}O$) relative to V-PDB (Vienna–Pee Dee belemnite) and analytical precision was ±0.06‰.
37. D. Paillard, L. Labeyrie, P. Yiou, Eos 77, 379 (1996).
38. E. Bard, G. M. Raisbeck, F. Yiou, J. Jouzel, Earth Planet. Sci. Lett. 150, 453 (1997).
39. We thank two anonymous reviewers and R. Gill for thoughtful review and discussion, T. Janecek and Y. Guyodo for analytical assistance, and S. Harris, C. Page, J. Abreu Sierra, E. May Bote, and R. Medina Gonzalez for logistical field support. Radiocarbon analyses were made at the Center for AMS under the auspices of the U.S. Department of Energy by University of California Lawrence Livermore National Laboratory Contract W-7405-Eng-48. Supported by the U.S. National Science Foundation (EAR-9709314), National Geographic Society, University of Florida Opportunity Fund, and the British Broadcasting Corporation. Publication L-0001 of the Land Use and Environmental Change Institute.

27 November 2000; accepted 28 March 2001

Origin and Environmental Setting of Ancient Agriculture in the Lowlands of Mesoamerica

Kevin O. Pope,[1]* Mary E. D. Pohl,[2] John G. Jones,[3] David L. Lentz,[4] Christopher von Nagy,[5] Francisco J. Vega,[6] Irvy R. Quitmyer[7]

Archaeological research in the Gulf Coast of Tabasco reveals the earliest record of maize cultivation in Mexico. The first farmers settled along beach ridges and lagoons of the Grijalva River delta. Pollen from cultivated Zea appears with evidence of forest clearing about 5100 calendar years B.C. (yr B.C.) [6200 ^{14}C years before the present (yr B.P.)]. Large Zea sp. pollen, typical of domesticated maize (Zea mays), appears about 5000 calendar yr B.C. (6000 yr B.P.). A Manihot sp. pollen grain dated to 4600 calendar yr B.C. (5800 yr B.P.) may be from domesticated manioc. About 2500 calendar yr B.C. (4000 yr B.P.), domesticated sunflower seeds and cotton pollen appear as farming expanded.

Mesoamerica is one of the cultural regions of the world that served as a cradle for plant domestication. Early research on plant domestication focused on the semi-arid highlands of Mexico, where preservation of plant macrofossils in dry caves was optimal (1, 2). The rich paleoethnobotanical data recovered from caves formed the basis for the hypothesis that the highland region was the center of domestication in Mesoamerica. Evidence for early agriculture has been more difficult to find in the lowlands, where humid conditions typically lead to poor plant preservation. Thus, the role of the humid tropical areas of Mesoamerica in plant domestication has remained terra incognita, although this region gave rise to one of the New World's first complex societies: the Gulf coast Olmec circa (ca.). 1300 calendar yr B.C. (3).

Our research traces the interaction of early lowland farmers with their dynamic coastal lagoon and estuarine environment in the Gulf coast of Mexico. Fieldwork focused on the small site of San Andrés (Fig. 1), located 15 km south of the Gulf of Mexico and 5 km northeast of the major Middle Formative Olmec center of La Venta in western Tabasco, Mexico (4). This part of Tabasco is hot and humid, with a marked seasonality in rainfall [a total of 800 mm from September to October, versus a total of 200 mm from January to May (5)]. The ecology and geomorphology of the coastal zone are characterized by mangroves bordering bar-

[1]Geo Eco Arc Research, 16305 St. Mary's Church Road, Aquasco, MD 20608, USA. [2]Department of Anthropology, Florida State University, Tallahassee, FL 32306, USA. [3]Department of Anthropology, Texas A&M University, College Station, TX 77843, USA. [4]New York Botanical Garden, Bronx, NY 10458, USA. [5]Department of Anthropology, Tulane University, New Orleans, LA 70118, USA. [6]Instituto de Geología, Ciudad Universitária, Mexico, D. F. 04510, Mexico. [7]Florida Museum of Natural History, Department of Natural History, Gainesville, FL 32611, USA.

*To whom correspondence should be addressed. E-mail: kpope@starband.net